Original Research

Advances in Structural Engineering

Advances in Structural Engineering
1–19

DOI: 10.1177/1369433217737115
journals.sagepub.com/home/ase
SAGE

Probabilistic seismic demand assessment of steel frames braced with reduced yielding segment buckling restrained braces

Ebrahim Afsar Dizaj[1], Nader Fanaie[2] and Arash Zarifpour[3]

Abstract

Buckling-restrained braces have adequate seismic performance characteristics such as high energy absorption due to their symmetric behaviour in compression and tension. However, low post-yield stiffness is one of the main disadvantages of these braces. The stiffness values of buckling-restrained brace frames can highly degrade when the core segments are yielded. Reducing the length of the yielding segments of buckling-restrained braces is being proposed and investigated by many researchers, considering the high strain capacity of steel in the post-elastic region. This article focuses on a type of buckling-restrained brace called reduced yielding segment buckling restrained brace or in short, 'reduced length buckling restrained brace'. In such frames, the length of the yielding part is reduced and placed in one end of the brace element. In this research, the seismic performances of the above-mentioned buckling-restrained braces were investigated through probabilistic approach and compared with those of conventional buckling-restrained braces. Their performances were quantitatively assessed in terms of two limit states, immediate occupancy and collapse prevention. The fragility curves, the mean annual limit states frequencies and the seismic demand hazard curves of the frames were plotted using probabilistic seismic demand analysis. According to the results obtained for immediate occupancy limit state, the frames braced with reduced length buckling restrained braces show better seismic performances compared to those braced with conventional buckling-restrained braces. However, for collapse prevention limit state, it is hard to comment accurately because in some cases, reduced length buckling restrained braced frames show enhanced seismic performance while in other cases, conventional ones exhibit improved response.

Keywords

incremental dynamic analysis, probabilistic seismic demand analysis, reduced length buckling restrained brace, seismic demand hazard curve, seismic performance

Introduction

Concentrically braced frames (CBFs) did not show acceptable performance during the earthquakes that happened in recent decades; beams and columns were damaged in the Kobe (1995), Northridge (1994) and Mexico (1985) earthquakes (Di Sarno and Elnashai, 2008). Therefore, they have been replaced with buckling-restrained braced frames (BRBFs) in the practical applications. BRBFs are steel seismic load resisting systems that are widely used in many parts of the world nowadays because of their efficiencies. They have been used also for seismic retrofitting of existing reinforced concrete frames (Di Sarno and Manfredi, 2012). In buckling-restrained braces (BRBs), by preventing brace buckling, high amount of energy is dissipated in every single cycle, and a symmetric and stable hysteresis curve is achieved (Bai and Ou, 2016).The buckling-restrained brace has a core plate through which the axial force is transmitted; its outer surface is covered with a restraining part to prevent buckling. An unbounded material or clearance is provided between the core plate and the restraining part to prevent the transmission of axial force from the former to the latter. Thus, the buckling-restrained brace can provide a nearly equal yield axial force in tension and compression, and supply stable hysteresis characteristics.

Reducing the core length (yielding segment) leads to the development of overstrength in the structure and

[1]Faculty of Engineering, University of Guilan, Rasht, Iran
[2]Department of Civil Engineering, K. N. Toosi University of Technology, Tehran, Iran
[3]Department of Civil Engineering, Islamic Azad University, Tehran, Iran

Corresponding author:
Ebrahim Afsar Dizaj, Faculty of Engineering, University of Guilan, Rasht, Iran.
Email: ebrahim_afsar@live.com

Table 1. Summary of some studies on BRB with reduced core length (Shemshadian et al., 2011a).

Researcher (year)	Location	L_c/L (%)	Model	Max. strain (%)
Tremblay et al. (2006)	Canada	25	Experimental and analytical	3.40
Mirghaderi and Ahlehagh (2008)	Iran	35	Analytical	4.30
Ning Ma et al. (2009)	China	20	Experimental	3.4.
	Italy	40	Experimental	3.50
Razavi and Mirghaderi (2009)	Iran	20–40	Analytical and experimental	3–4
Di Sarno and Manfredi (2010)	Italy	20	Analytical	1.50
Di Sarno and Manfredi (2012)	Italy	25	Experimental	0.40

BRB: buckling-restrained brace.

increases post-yield stiffness of the braces. Therefore, the lack of high post-elastic stiffness of conventional BRBs could be compensated for. The above advantages motivated researchers to investigate the possibility of reducing the length of the core in BRBs: most of these researches were carried out in recent years (Shemshadian et al., 2011a). A summary of the aforementioned studies is shown in Table 1. In this Table, L_c/L is ratio of the yielding core length to the whole brace length.

Shemshadian et al. (2011b) suggested the reduction of the yielding segment of BRB with details similar to that of Di Sarno and Manfredi (2010), which was used to retrofit non-ductile reinforced concrete (RC)–framed buildings. In this BRB type, the length of the yielding segment is reduced; that is, it is smaller than that of the conventional one. In the reduced length BRB, this segment is placed at one end of the brace element, while in the conventional BRBs, they are placed in the middle of the brace length. The mentioned segment acts as a structural fuse and in certain conditions, after severe earthquakes, only the damaged fuse is replaced with a new one (only at the end of the brace) and not the entire brace length. In such BRBs, each brace element has two parts: (1) yielding segment and (2) elastic part or non-yielding segment. The yielding segment as a displacement control part is a small BRB yielded in tension and compression, restrained against buckling, and its core cross section is smaller than that of the elastic part. The elastic part has a greater cross section compared to the yielding segment and is not restrained against buckling. It is expected to remain elastic and therefore is the force controlling part. One of the main criteria in designing such systems is to prevent the brace from global buckling without using any restraining mechanism in the non-yielding part (Shemshadian et al., 2011b). Figure 1 shows schematic application of the reduced yielding segment BRB in inverted-V shape (Razavi et al., 2014) and three-dimensional view of the brace detailing. Razavi et al. (2011, 2014) proposed a procedure for designing reduced length BRBF system and tested two

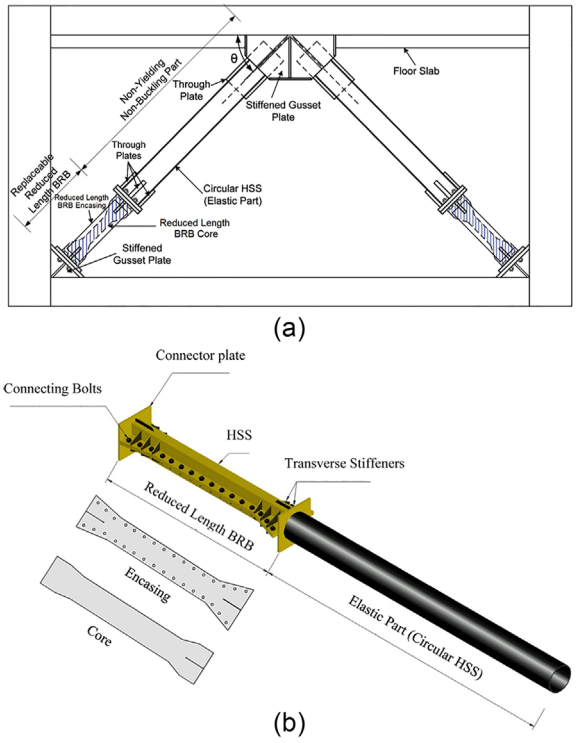

Figure 1. BRB with reduced yielding segment: (a) application in inverted-V shape and (b) 3D view of the brace detailing.

different detailings of the reduced BRB, case 1 – reduced length BRB placed at the end of the brace element and case 2 – reduced length BRB placed on the middle of the brace, and concluded that in the case 1 higher buckling capacity is achieved.

According to their results, there is no significant difference between designing the suggested BRB and a common BRBF. Furthermore, the recommended system showed high potential in reducing residual drifts due to its proper inelastic stiffness (Razavi et al., 2011). In author's another research (Fanaie and Afsar Dizaj, 2014), response modification factor was evaluated for the frames braced with this type of BRBs and compared to the conventional types. According to the

obtained results, the values of response modification, ductility and overstrength factors are higher in the reduced yielding segment BRBFs compared to those of conventional ones. It means that the new BRBs show higher capacities in absorbing earthquake energy and can replace ordinary BRBs. The main objective of this research is to evaluate the seismic performance of reduced length BRBFs and compare them to that of conventional BRBFs using a probabilistic method for the treatment of both randomness and uncertainty. This method is generally known as the probabilistic seismic demand analysis (PSDA). The performance of structures was assessed through incremental dynamic analysis (IDA) in two different levels, collapse prevention (CP) and immediate occupancy (IO). First-mode 5%-damped spectral acceleration (Sa (T_1, 5%)) and peak inter-storey drift ratio ($\theta_{\max}$) were selected as the representative terms for ground motion intensity measure (IM) and engineering demand parameter (EDP), respectively. The probability of structural failure in meeting the desired performance is evaluated through limit state (limit states) analysis of IDA data.

Design procedure of the reduced yielding segment BRB

Reduced core length BRB elements were designed based on the procedure presented by Razavi et al. (2011). Figure 2 shows the geometric dimensions of the reduced yielding segment BRB for design procedure. The cross-sectional area of the yielding part (A_2) is specified according to the strength needed. AISC 341-05 requires that the buckling-restraining system shall limit local and overall buckling of steel core, and the restraining system shall not be permitted to buckle within deformations corresponding to 2.0 times the design storey drift (Δ_m). The minimum needed length of the yielding part (L_2) is determined based on the maximum brace axial displacement at the inter-storey drift of $2\Delta_m$ and the maximum allowable strain ($\varepsilon_{\max}$) according to equation (1)

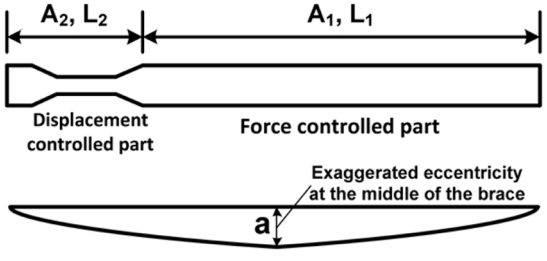

Figure 2. Geometric dimensions for design procedure (Razavi et al., 2011).

$$L_2 \geqslant \frac{2\Delta_{bm}}{\varepsilon_{\max}} \tag{1}$$

In this equation, Δ_{bm} is brace axial displacement corresponding to design storey drift, Δ_m. The maximum allowable strain, $\varepsilon_{\max}$, is taken as 3.5% (Razavi et al., 2011). Furthermore, reducing BRB core length might raise concerns about low-cycle fatigue (LCF) failure. However, this criterion has been considered in the design procedure of the reduced length BRB by Razavi et al. (2014). According to Razavi et al. (2014), to limit strain amplitudes and prevent LCF failure, the length of the core was defined so that using the rules of Nakamura et al. (2000) and Miner (1945), the reduced length BRB be safe from LCF failure. More details are presented in the study of Razavi et al. (2014). Razavi et al. (2011) have recommended to keep the ratio of the yielding core length to the whole brace length from 0.15 to 0.35 in order to save the structure from the effects of LCF failure. In this study, this ratio is taken as 0.25 which is the mean value of the proposed range. To design the non-yielding part of the brace, first the equation suggested by Watanabe et al. (1988) for avoiding the buckling of BRBs is checked

$$\frac{P_{cr}}{P_y} \geqslant 1.5, \; P_{cr} = \frac{\pi^2 EI}{L^2} \tag{2}$$

where P_{cr} is the elastic buckling force of the brace, and P_y is the yielding force of the yielding part. I is the moment of inertia of non-yielding part, and L is the total length of the brace (work point to work point). In the next step, an initial lateral deflection, a, representing the maximum allowable eccentricity of a compression member in the middle of the brace is assumed according to AISC 303-10 (2010), Figure 2. The maximum lateral deformation of the brace at the inter-storey drift of $2\Delta_m$ is calculated by the following stability equation

$$\Delta_{\max} = \frac{a}{1 - P/P_{cr}} \tag{3}$$

where P is the maximum expected force that the yielding part can develop at the inter-storey drift of $2\Delta_m$. The following equations describe the maximum axial and bending stresses in the middle of brace, respectively

$$f_a = \frac{P}{A_1}, \; f_b = \frac{P\Delta_{\max}}{S} \tag{4}$$

where A_1 and S are the cross-sectional area and the section modulus of the non-yielding part, respectively. The combined stress caused by beam–column action should be controlled in the middle of the brace using

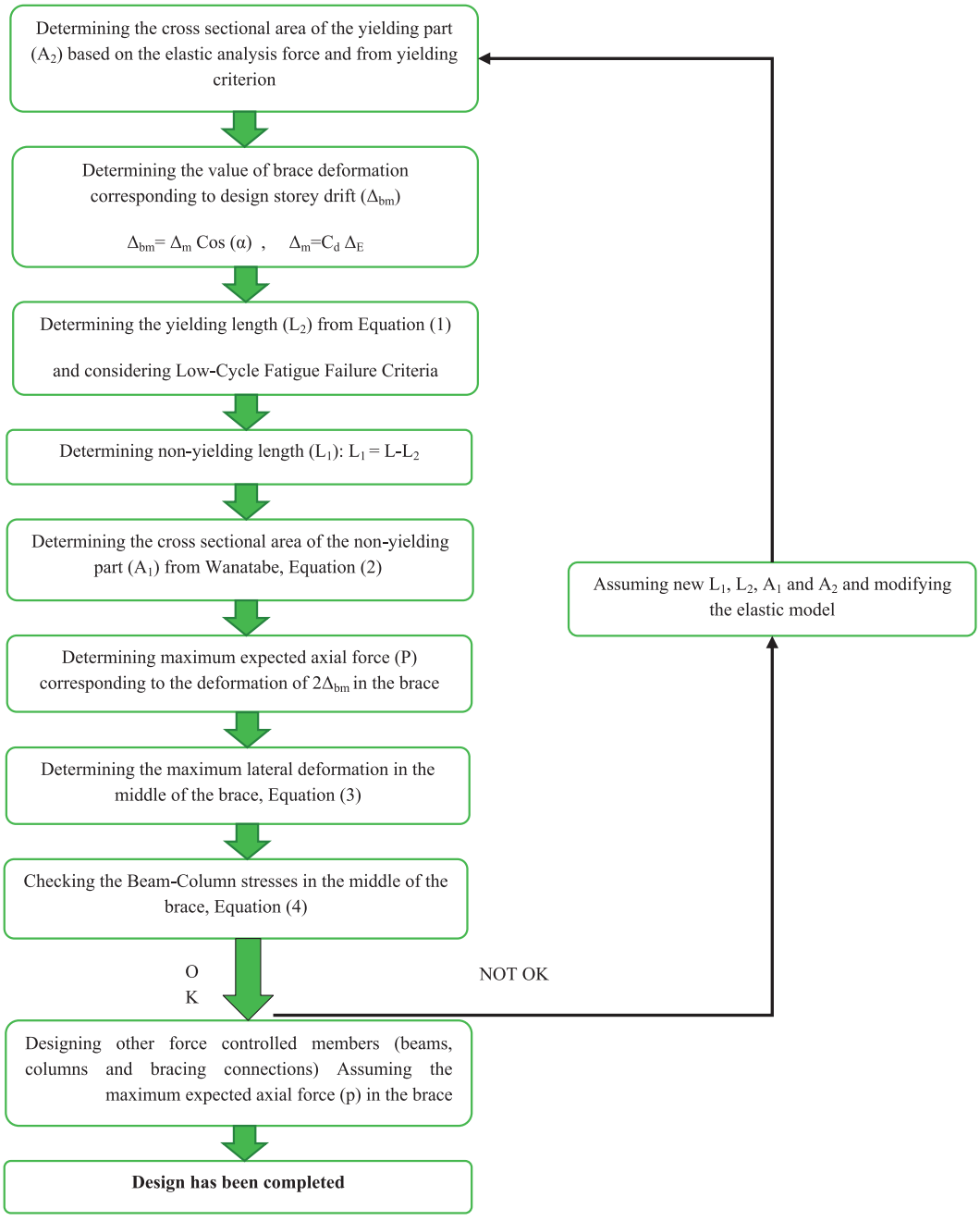

Figure 3. Design procedure of the BRB system with reduced core length (Razavi et al., 2011).

AISC 360-10. In Figure 3, the step-by-step design procedure of this type of BRB is shown in a flowchart.

The studied models

As mentioned earlier, this research is meant to evaluate the probabilistic seismic performance of reduced yielding segment BRB and compare it with that of conventional BRB. For this purpose, 3-, 6-, 9- and 12-storey frames were considered with 5-m bay length and two different BRB types, conventional and reduced length BRBs. They were designed in chevron inverted-V and diagonal configurations (totally 16 frames), according to the Iranian Earthquake Resistant Design Code and *Iranian National Building Code, Part 10, Steel Structure Design* (Ministry of Housing and Urban Development, 2008). Figure 4 shows plan and elevation of the modelled frames. The storey height of the models was taken as 3 m. The equivalent lateral static forces were applied on all storey levels for the member

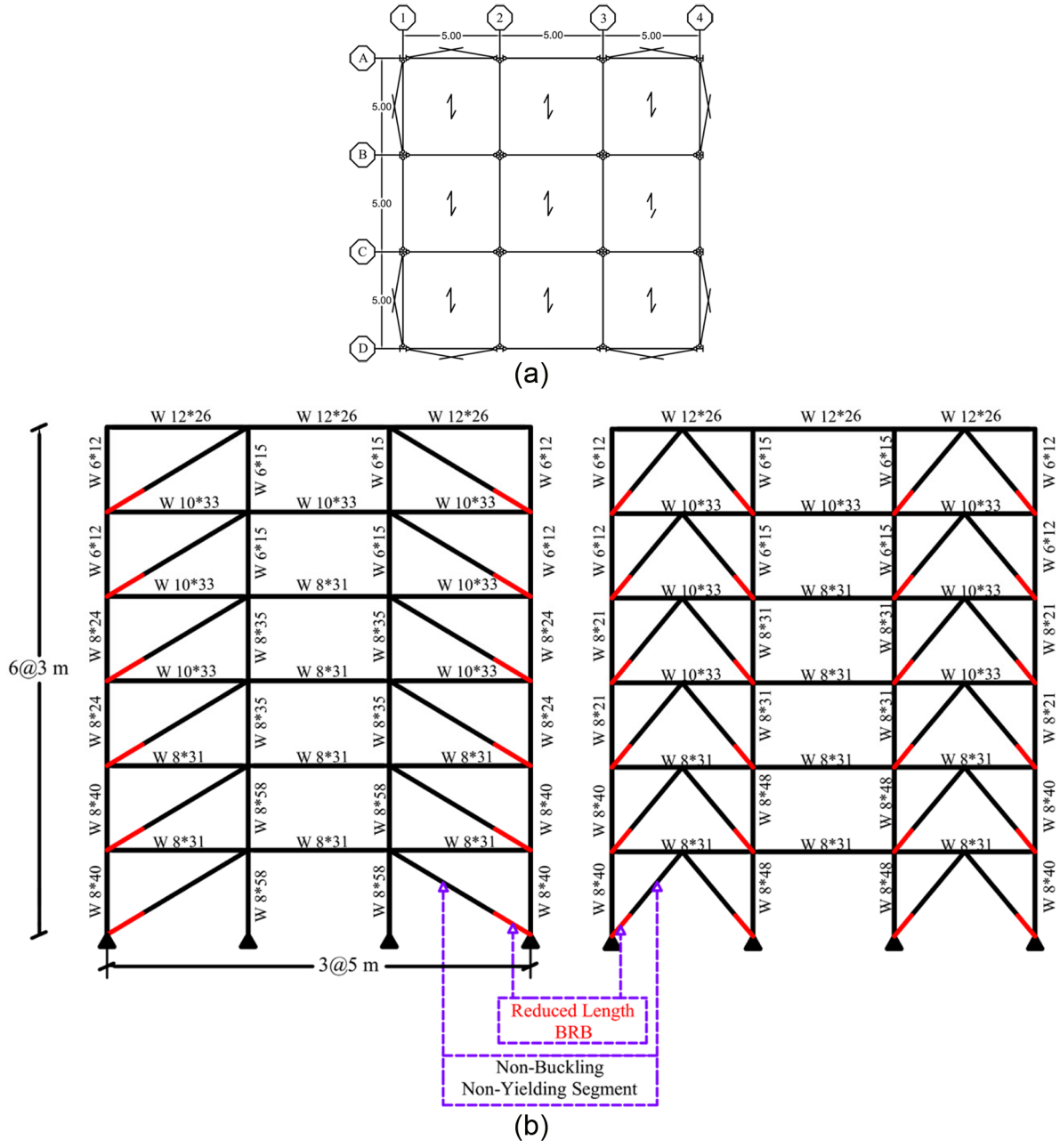

Figure 4. (a) Plan of the frames and (b) geometries of the extracted two-dimensional frames.

design subjected to earthquake. These forces were calculated according to the provisions stated in Iranian Earthquake Code BHRC Standard 2800 (2005). The dead and live loads were considered as 600 and 200 kgf/m^2, respectively, for the floors, and 550 and 150 kgf/m^2, respectively, for the roof. Moreover, the dead load caused by peripheral walls was considered as 800 kgf/m. The design base shear is computed as follows

$$V = CW, C = \frac{ABI}{R} \quad (5)$$

where V is base shear, C is seismic coefficient, W is equivalent weight, A is design base acceleration, B is response coefficient, I is importance factor and R is response modification factor of the structure. In designing the frame, the importance factor (I) was taken as 1, response modification factor (R) as 7 and design base acceleration (A) as 0.35. It was assumed that the braces were pinned at both ends. Furthermore, reduced length BRB elements were designed based on the procedure presented in the previous section. According to American Institute of Steel Construction (AISC) (2005) seismic provisions, axial design strength

Table 2. Brace design details of three-storey frames.

Configuration	No. of storeys	Non-yielding part Pipe (outer diameter × thickness) (cm)	Ratio of yielding part length to whole brace length	Yielding core cross section (cm^2)
Inverted-V	3	14 × 0.6	0.25	6.5
	2	16 × 0.62	0.25	9.7
	1	18 × 0.64	0.25	12.9
Diagonal	3	18 × 0.8	0.25	9.7
	2	20 × 0.9	0.25	12.9
	1	20 × 1.1	0.25	19.4

Table 3. Brace design details of six-storey frames.

Configuration	No. of storeys	Non-yielding part Pipe (outer diameter × thickness) (cm)	Ratio of yielding part length to whole brace length	Yielding core cross section (cm^2)
Inverted-V	6	18 × 0.64	0.25	6.5
	5	22 × 0.68	0.25	12.9
	4	22 × 0.68	0.25	12.9
	3	22 × 0.68	0.25	16.1
	2	22 × 0.7	0.25	19.3
	1	22 × 0.7	0.25	19.3
Diagonal	6	20 × 1.1	0.25	9.7
	5	24 × 1.2	0.25	16.1
	4	24 × 1.2	0.25	19.4
	3	24 × 1.2	0.25	22.6
	2	25 × 1.2	0.25	25.8
	1	25 × 1.2	0.25	29.0

of beams and columns are checked against the required axial strength induced by the adjusted BRB strengths at $2\Delta_{bm}$. Tables 2 to 5 present the brace design details of 3-, 6-, 9- and 12-storey frames braced with reduced yielding segment BRB, respectively. The conventional BRB is designed using core cross section by one element. The actual length of the steel core is smaller than the work-point-to-work-point length of the brace. As a result, the actual stiffness of the brace is greater than that computed using only steel core area. Accordingly, the effective stiffness of BRB is defined as 1.4 times the stiffness computed using only the steel core. This is consistent with many actual designs (López and Sabelli, 2004).

Modelling the frames

The frames were modelled using OpenSees (Mazzoni et al., 2007), a finite element software specified for designing structures that are prone to earthquakes. Here, two-dimensional (2D) frame corresponding to *A*-axis of the plan was modelled using OpenSees in order to perform IDA. To take into account the P–Δ effects of the gravity frames on seismic response of the frames, half of total gravity load of each floor is applied to a dummy column. The column and beam elements as well as the sections were modelled using nonlinear beam–column element and fibre section. In this study, the Giuffre–Menegotto–Pinto (GMP) (Menegotto and Pinto, 1973) model implemented in OpenSees as the steel02 material model is used to model the uniaxial stress–strain response of steel. The GMP model employs a smooth transition curve that asymptotically approaches bilinear tension and compression response envelopes; this enables simulation of the Bauschinger effect. To define the Steel02, the required parameters are yield strength, elastic modulus and hardening ratio of the steel. To design beams and columns, ASTM A992 material with yield strength of 3515.3 kg/cm^2 (50 ksi) and elasticity modulus of 2,038,902 kg/cm^2 (29,000 ksi) is considered. The conventional BRB is modelled by one equivalent element using corotational truss element. The ASTM A36 material with yield strength of 2531 kg/cm^2 (36 ksi) and elasticity modulus of 2,038,902 kg/cm^2 (29,000 ksi) is used to design BRBs; the strain hardening is considered as 1%.Two elements, yielding part and non-yielding part, were used to model the

Table 4. Brace design details of nine-storey frames.

Configuration	No. of storeys	Non-yielding part Pipe (outer diameter × thickness) (cm)	Ratio of yielding part length to whole brace length	Yielding core cross section (cm^2)
Inverted-V	9	22 × 0.65	0.25	6.5
	8	24 × 0.75	0.25	9.7
	7	26 × 0.8	0.25	12.9
	6	26 × 0.88	0.25	16.1
	5	26 × 0.88	0.25	19.4
	4	26 × 0.88	0.25	19.4
	3	26 × 0.9	0.25	22.6
	2	26 × 0.9	0.25	22.6
	1	26 × 0.9	0.25	22.6
Diagonal	9	24 × 1.2	0.25	9.7
	8	26 × 1.2	0.25	12.9
	7	28 × 1.4	0.25	19.4
	6	28 × 1.4	0.25	22.6
	5	28 × 1.4	0.25	25.8
	4	28 × 1.4	0.25	29.0
	3	28 × 1.5	0.25	32.3
	2	28 × 1.5	0.25	32.3
	1	28 × 1.5	0.25	35.5

Table 5. Brace design details of 12-storey frames.

Configuration	No. of storeys	Non-yielding part Pipe (outer diameter × thickness) (cm)	Ratio of yielding part length to whole brace length	Yielding core cross section (cm^2)
Inverted-V	12	26 × 1	0.25	6.5
	11	28 × 1.3	0.25	12.9
	10	28 × 1.3	0.25	12.9
	9	28 × 1.3	0.25	16.1
	8	28 × 1.4	0.25	19.4
	7	28 × 1.4	0.25	19.4
	6	28 × 1.4	0.25	22.6
	5	28 × 1.4	0.25	22.6
	4	28 × 1.41	0.25	25.8
	3	28 × 1.41	0.25	25.8
	2	28 × 1.41	0.25	25.8
	1	28 × 1.41	0.25	25.8
Diagonal	12	26 × 1.6	0.25	9.7
	11	28.5 × 1.6	0.25	12.9
	10	30 × 1.7	0.25	16.1
	9	30 × 1.7	0.25	19.4
	8	30 × 1.7	0.25	22.6
	7	30 × 1.8	0.25	25.8
	6	30 × 1.8	0.25	29.0
	5	30 × 1.8	0.25	32.3
	4	30 × 1.8	0.25	32.3
	3	31 × 1.8	0.25	35.5
	2	31 × 1.8	0.25	35.5
	1	31 × 1.8	0.25	38.7

reduced yielding segment BRB. The former was modelled with steel 02 material model (like conventional BRB) and the elastic part by hysteretic material model to define buckling limitation point in pressure. The elements of both parts were nonlinear beam–column element. The corotational coordinate transformation (CorotCrdTransf) object was used for all elements.

Table 6. Ground motions used in IDA.

Earthquake	Station	Date	PGA (g)
Cape Mendocino	1806, Rio Dell Overpass-FF	25 April 1992	0.549
Chi-Chi, Taiwan	CHY080	20 September 1999	0.968
Coyote Lake	Gilroy Array 3	6 August 1979	0.434
Kobe	KJMA	16 January 1995	0.821
Kocaeli, Turkey	Sakarya	17 August 1999	0.376
Landers	Coolwater	28 June 1992	0.417
Loma Prieta	Corralitos	18 October 1989	0.644
Morgan Hill	Anderson Dam	24 April 1984	0.423
N. Palm Springs	N. Palm Springs	8 July 1986	0.694
Northridge	Santa Monica	17 January 1994	0.883
Parkfield	Temblor pre-1969	28 June 1966	0.357
San Fernando	Lake Hughes #12	9 February 1971	0.366
Superstition Hills	USGS station 5051	24 November 1987	0.455
Victoria, Mexico	UNAM/UCSD station 6604	9 June 1980	0.621
Whittier Narrows	Obregon Park	1 October 1987	0.45
Tabas	Tabas, LN	16 September 1978	0.836
Bam	Bam	26 December 2003	0.799

IDA: incremental dynamic analysis; PGA: peak ground acceleration.

IDA of frames

The idea on the base of the IDA is to multiple dynamic analyses on the same structure, scaling each time the intensity, in order to cover the full behaviour (Vamvatsikos and Cornell, 2002). Typically, one set of accelerograms (natural or artificial) is selected; the dynamic analyses are performed and for each of them, the performance of the structure is investigated considering some key factors (e.g. the top displacement and hysteresis loops at the base on the columns). Depending on the intensity level of the record chosen, the system can have an elastic behaviour or going deeply in the nonlinear range; from the other side, the use of a nonlinear static analysis gives, in a static way, a complete picture of the performance of the structure, from limited damage up to collapse (Titi, 2013). In this study, 17 natural ground motions were used for IDA. These ground motions are selected from famous worldwide earthquakes including two big earthquakes in Iran, Bam and Tabas, based on the soil type of the site, that is, shear wave velocities of all these sites correspond to the velocity in soil type II as presented by Iranian code for seismic design, BHRC Standard 2800 (2005). Details of these ground motions are presented in Table 6.

Before performing an IDA, two quantities must be selected, namely, the IM and the EDP or damage measure (DM). Proper selection of IM and EDP is important in performing IDA. A properly selected IM will yield smaller scattering in the statistical distribution of IDA data. EDP should be selected according to the expected function and dominant failure mechanism of the structure. In this study, first-mode 5%-damped spectral acceleration (Sa (T_1, 5%)) was chosen as IM and maximum inter-storey drift ratio ($\theta_{\max}$) as EDP. Hunt and fill algorithm was used to establish an automated still time-efficient procedure for IDAs (Jalali et al., 2012). Figure 5 shows the IDA curves of three-storey frames (as example) for all records, along with summarized curves. Figure 6 presents the median IDA curves of the frames braced with conventional and reduced length BRBs, inverted-V and diagonal braces. As expected, the IDA experiences a lower IM for a constant value of EDP with increasing building height. This is caused by the Sa capacity which is lower in tall buildings compared to short ones.

The median of each graphs of Figure 6 is plotted in Figure 7 to have a single curve for each type of brace. Figure 8 shows the median of the median curves for two single IDA curves related to conventional BRBs and reduced length BRBs for better comparison. As can be seen in Figure 8, for a constant EDP value, IDA experiences a greater IM for reduced length BRB. This means that the Sa capacity of reduced BRBFs is higher compared to that of conventional BRBFs.

Fragility curves

After performing IDAs, the fragility curves were extracted to evaluate the probability of failure so as to meet the desired performance of the structures. These curves schematically illustrate the relationship between the probability of structural damage and earthquake IM. The fragility curves are generally modelled by a lognormal cumulative distribution function (CDF). The fragility curves were constructed in terms of

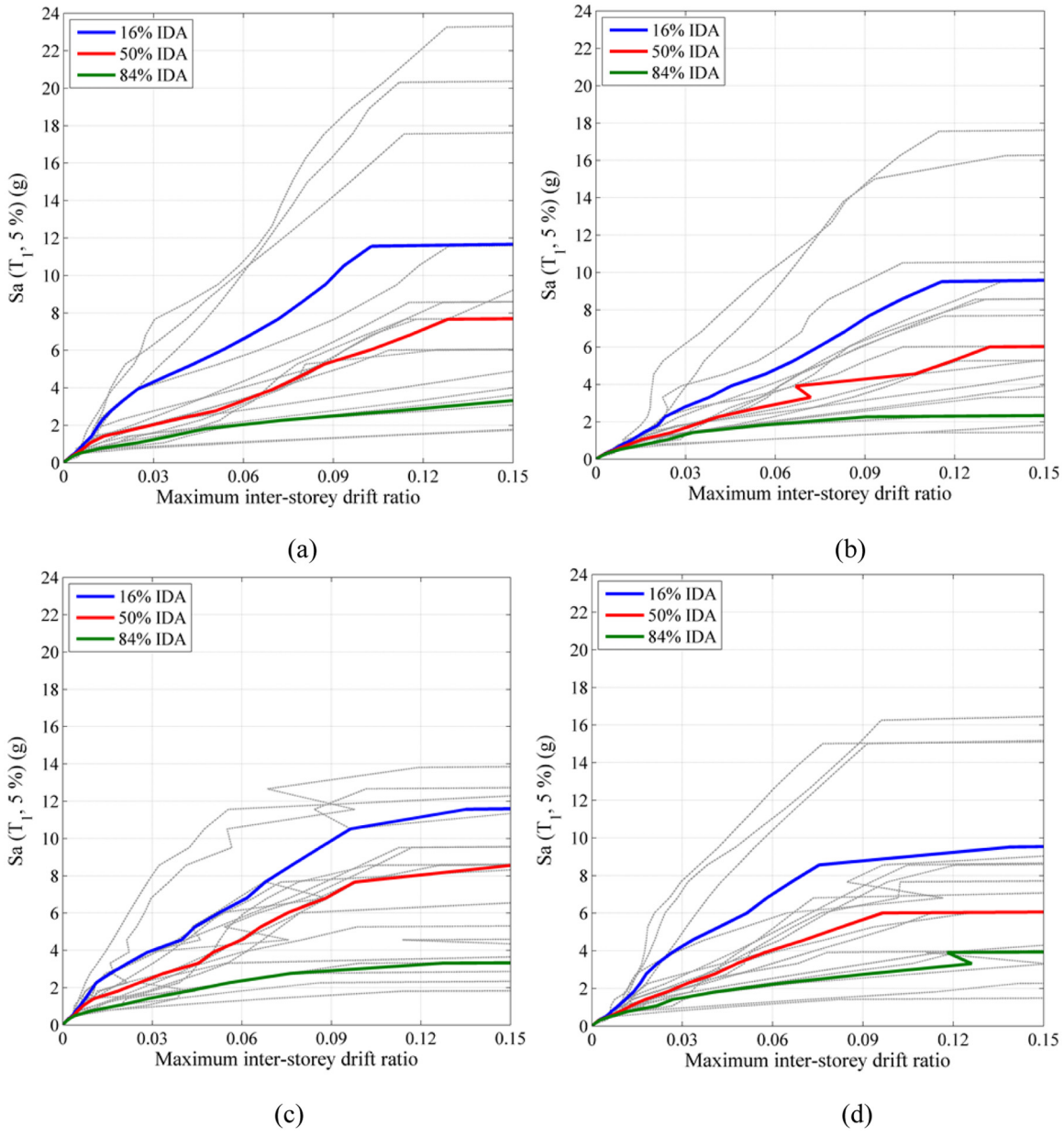

Figure 5. Full and percentile IDA curves of three-storey frames: (a) inverted-V – conventional BRB, (b) diagonal – conventional BRB, (c) inverted-V – reduced length BRB and (d) diagonal – reduced length BRB.

spectral acceleration at the fundamental periods of the structures and expressed in the form of two-parameter lognormal distribution functions. With the conditional probability of EDP exceeding x, given that the spectral acceleration (Sa (T_1)) equals y, fragility function is defined as follows (Papailia, 2011; Tonekabonipour, 2013)

$$\int P[EDP \geqslant x | Sa(T_1) = y] = \Phi\left(\frac{\ln(x) - \mu_{\ln}}{\sigma_{\ln}}\right) \quad (6)$$

where Φ is the CDF of the standard normal distribution, x is lognormal distributed spectral acceleration and $\mu_{\ln}$ is the mean of the variable natural logarithm.

The probability of occurrence was evaluated for two limit states: CP and IO. $\theta_{\max}$ (maximum inter-storey drift ratio) value is limited to 10% for determining the CP state, along with setting a slope limit equal to 20% of the initial elastic tangent for IDA curves (Ariyaratana and Fahnestock, 2011; Choi et al.,2017; Fanaie and Ezzatshoar, 2014; Shin and Kim, 2016). $\theta_{\max}$ is limited to 2% for tracking IO limit states (Jalali

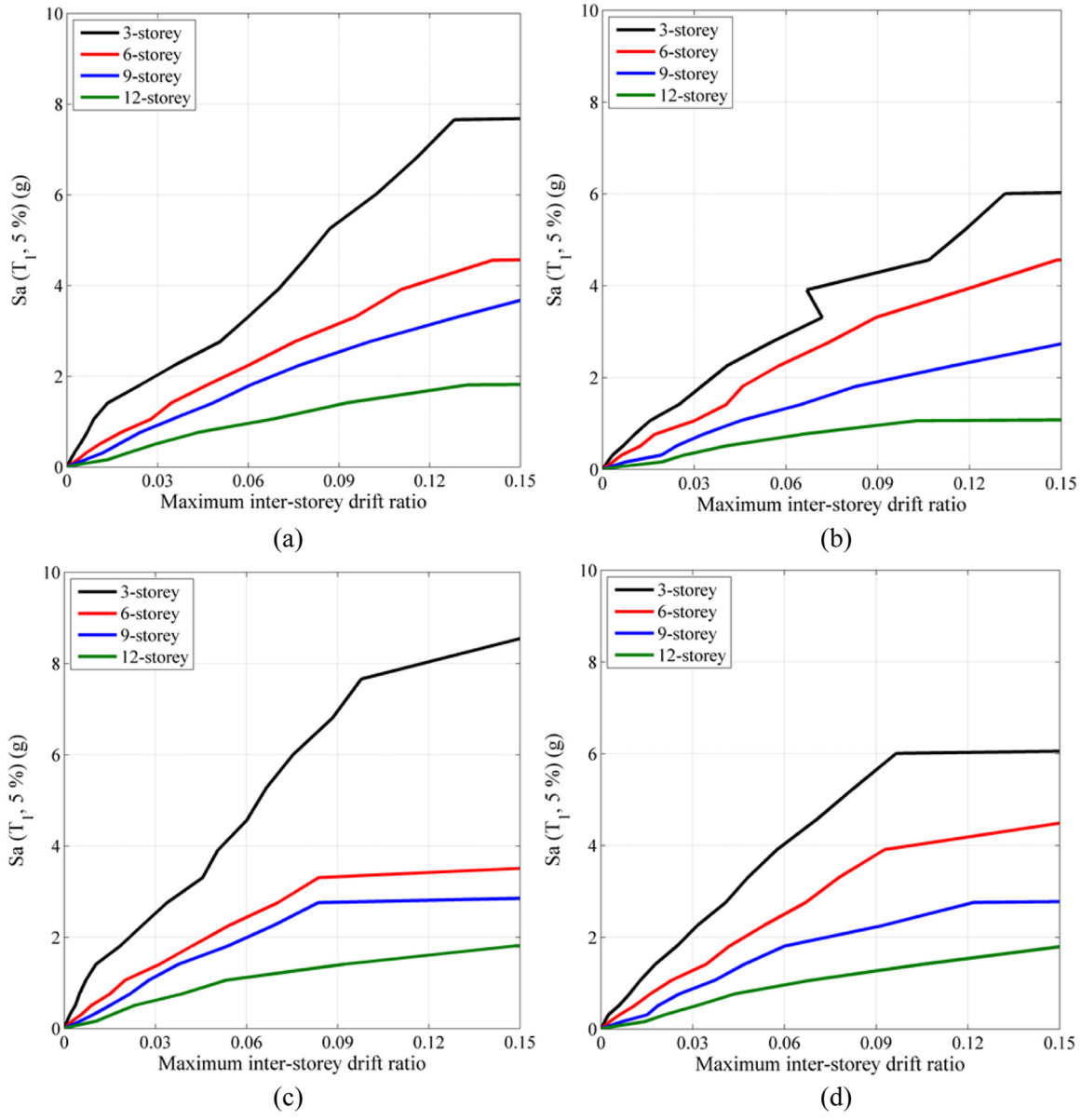

Figure 6. Median IDA curves of the frames: (a) inverted-V – conventional BRB, (b) diagonal – conventional BRB, (c) inverted-V – reduced length BRB and (d) diagonal – reduced length BRB.

et al., 2012). Figure 9 presents the fragility curves of all frames for IO limit states in terms of bracing type. According to this figure, the probability of exceedance of a specific *Sa* value is raised as the height of the building increases. This trend seems to be reasonable considering the fact that generally ductility of frames decreases as their height increases. For better comparison, in Figures 10 and 11, the fragility curves of conventional and reduced length BRBs are plotted in inverted-V and diagonal configurations, respectively. Based on these figures, the probability of exceedance of IO limit states is lower in the reduced length BRBFs for a specific *Sa* value, compared to that of conventional ones. This is because the lateral stiffness of the reduced length BRBFs is increased due to replacement of a large part of core segment by a greater section and as a result to achieve a same damage limit states, higher *Sa* is needed. Similarly, as can be seen in Figure 11, the probability of exceedance of CP limit states is lower for diagonal-reduced length BRBFs. However, it is difficult to estimate the response for the inverted-V bracing in CP limit states because the probability of exceedance of CP limit states for reduced length BRBs for some *Sa* values are lower in comparison to that of conventional BRBs, while for some other *Sa* values are higher.(Figure 10). Further investigations and experiments are needed to

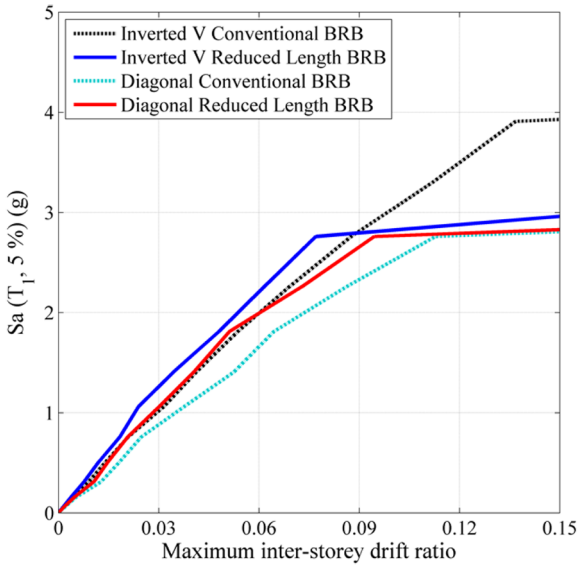

Figure 7. Median IDA curves of each type of BRBs.

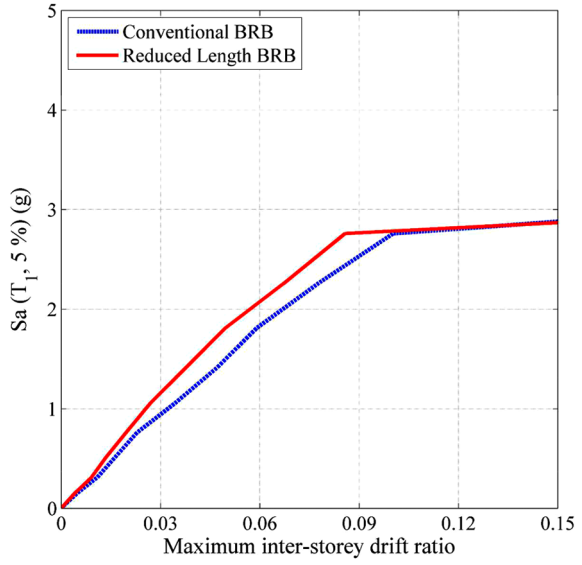

Figure 8. Median of Median IDA curves of each type of BRBs.

clarify the effectiveness of using inverted-V – reduced length BRBs in steel frames. This is an area for future research.

Table 7 present the *Sa* values corresponding to the failure probabilities of 16%, 50%, and 84% for different frames with two mentioned limit states. These quantities are valuable for specifying the seismic design of buildings regarding certain failure probability. According to Table 7, the *Sa* values corresponding to each failure probabilities are greater for reduced length BRBs, regarding each bracing configuration types in IO limit states and diagonal bracing in CP limit states. Concerning the inverted-V bracing in CP limit states, there is no distinct correlation between bracing type and *Sa* values corresponding to failure probabilities. It seems that the reduced length BRBs are more reliable than conventional BRBs. However, the results of inverted-V bracing in CP limit states, somehow do not imply the enhanced performance of reduced length BRBs in comparison with conventional ones. In the next part, probabilistic approach was used to compare more comprehensively the seismic performances of conventional and reduced length BRBs.

PSDA

Earthquakes and their consequences are inherently probabilistic, and it is necessary that earthquake engineers use a probabilistic procedure to assess the structural responses due to future ground motions (Mahdavipour and Deylami, 2014). PSDA is an interim element of the conceptual framework performance-based earthquake engineering (PBEE). PBEE is able to achieve diverse performance objectives (e.g. lower costs and time) that limit both structural and non-structural damage in various seismic hazard levels. The performance objectives are generally quantified as decision variables (DV) or EDPs, and annual probabilities of such variables exceed specific limit values in a seismic hazard environment of the site under consideration (Tang and Zhang, 2011). PSDA is embodied as follows (Mahdavi Adeli et al., 2011; Sehhati, 2008)

$$\lambda_{EDP}(x) = \int P[EDP \geqslant x|\mathrm{IM} = \mathrm{y}]|d\lambda_{IM}(y)| \qquad (7)$$

where $\lambda_{EDP}(x)$ is mean annual frequency (MAF) of engineering damage parameters (EDP) exceeding the x value; $\int P[EDP \geqslant x|\mathrm{IM} = \mathrm{y}]$ is the probability of EDP exceeding x given that IM equals y (fragility function); $d\lambda_{IM}(y)$ is MAF of occurrence of IM equal to y; and $\lambda_{IM}(y)$ is mean frequency of IM exceeding y (ground motion hazard), obtained from conventional probabilistic seismic hazard analysis (PSHA). A seismic hazard curve can be approximated as a linear function on a log–log scale for a relatively wide range of intensities and defined as follows (Jalayer and Cornell, 2003)

$$\lambda_{(Sa(T_1))} = k_0(Sa(T_1))^{-k} \qquad (8)$$

where $\lambda\ (Sa\ (T_1))$ is MAF of exceeding $Sa\ (T_1)$; and k_0 and k are parameters for defining the shape of the hazard curve. The seismic hazard curves used here are obtained from the study of Mahdavi Adeli (2005). He generated the uniform hazard maps for Tehran city and then plotted its seismic hazard curves. Figure 12

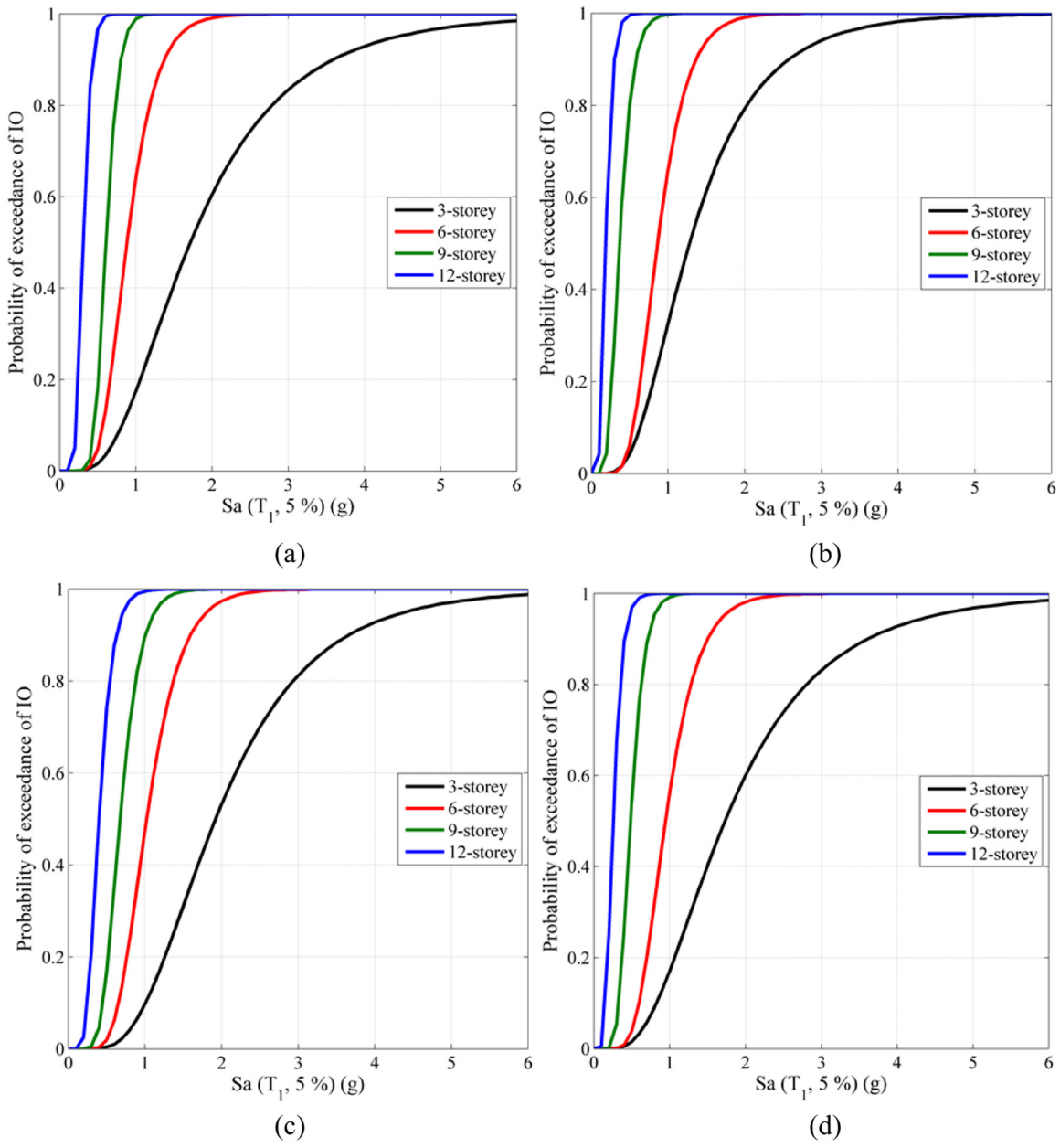

Figure 9. Fragility curves of all frames for IO limit state: (a) inverted-V – conventional BRB, (b) diagonal – conventional BRB, (c) inverted-V – reduced length BRB and (d) diagonal – reduced length BRB.

shows the simplified uniform hazard spectra for Tehran.

Table 8 presents the MAF of the frames for IO and CP limit states.

Seismic demand hazard curves

The outcome of PSDA is a seismic demand hazard curve. The PSHA yields the seismic hazard curve which provides the mean annual rate (MAR) of the IM Sa (T_1) exceeding any specified level at the site of interest (Faggella et al., 2013). In other words, seismic demand hazard curve gives the MAF of exceedance for different EDP levels. Accordingly, a formula similar to that of is applied to assume different levels of EDP. Figures 13 and 14 show the seismic demand hazard curves for all frames.

As can be seen in Figures 13 and 14, the demand hazard curves of diagonal-reduced length BRBs are beneath the curves of the conventional types, but for inverted-V – reduced length BRBs, these curves are below the corresponding curves of conventional BRBs

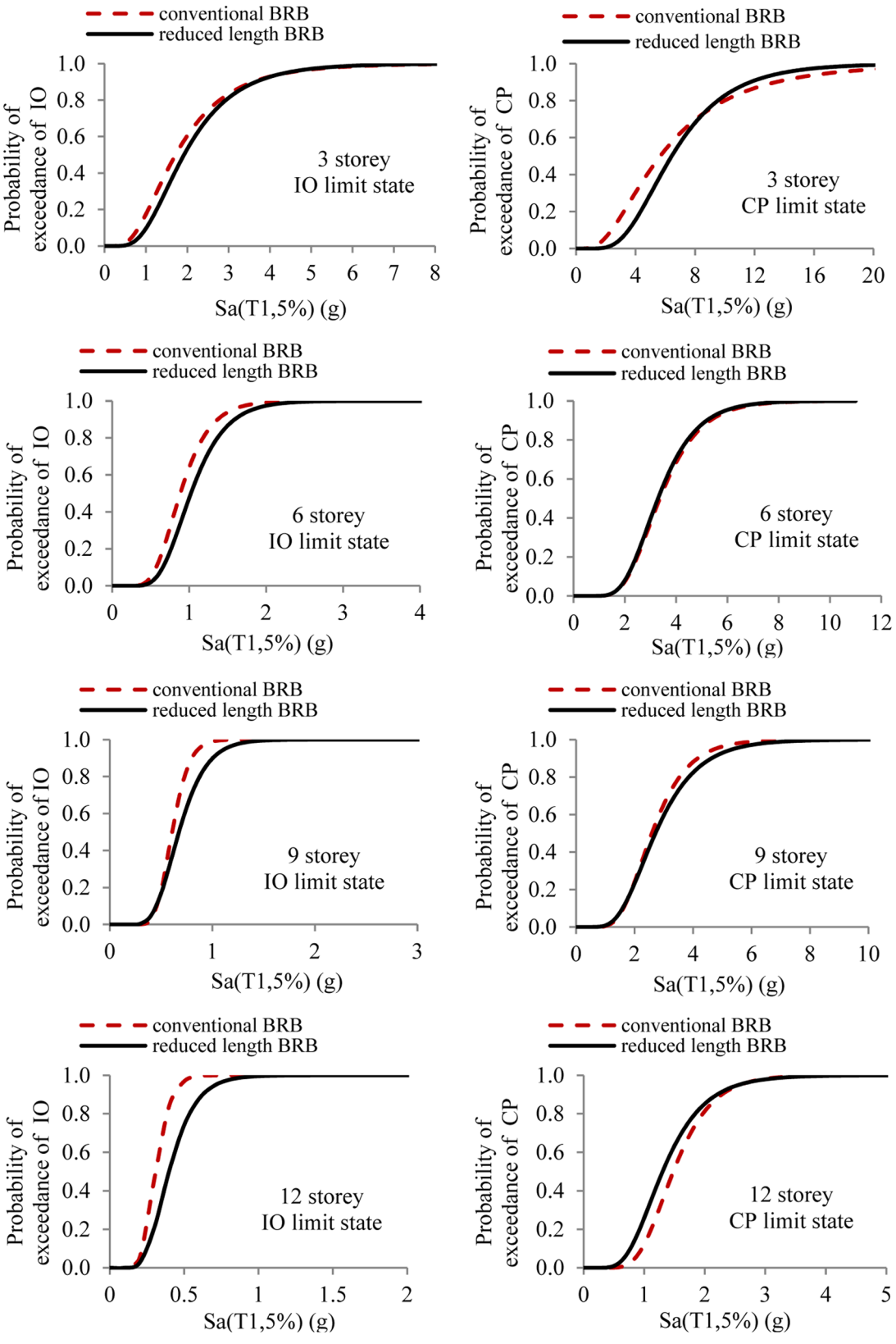

Figure 10. Fragility curves of inverted-V BRBFs.

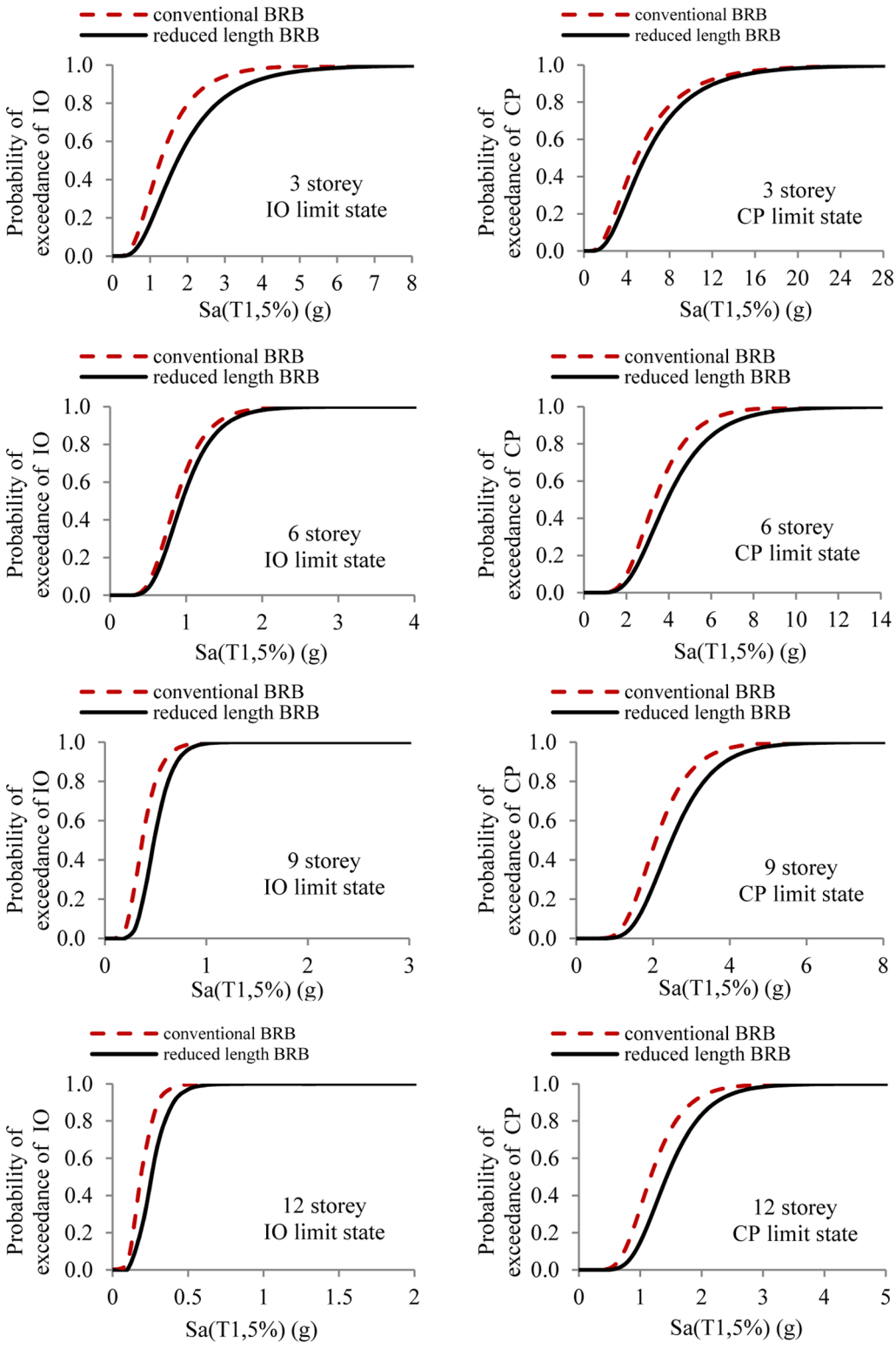

Figure 11. Fragility curves of diagonal BRBFs.

for certain EDPs and are above them for higher values of EDPs. These results are consistent with those achieved from Figures 10 and 11 and Table 7. That is to say that the MAF value is lower for a specific response level (i.e. θ_{max} value) in diagonal-reduced length BRBs, but this statement is not always true for

Table 7. *Sa* values, corresponding to different failure probabilities of the frames braced with inverted-V braces and diagonal braces.

Failure probability (%)		$(Sa)_{IO}$ (g)			$(Sa)_{CP}$ (g)		
		16%	50%	84%	16%	50%	84%
Inverted-V braces							
Conventional BRB	3 storey	0.97	1.72	3.04	2.89	5.66	11.06
	6 storey	0.63	0.89	1.25	2.35	3.37	4.81
	9 storey	0.49	0.61	0.76	1.80	2.59	3.74
	12 storey	0.23	0.31	0.40	1.06	1.48	2.07
Reduced length BRB	3 storey	1.16	1.92	3.17	4.04	6.43	10.23
	6 storey	0.72	1.02	1.44	2.31	3.30	4.69
	9 storey	0.49	0.68	0.92	1.79	2.71	4.11
	12 storey	0.27	0.40	0.57	0.86	1.30	1.96
Diagonal braces							
Conventional BRB	3 storey	0.74	1.28	2.20	2.60	4.89	9.19
	6 storey	0.61	0.87	1.23	2.26	3.35	4.95
	9 storey	0.25	0.37	0.53	1.47	2.07	2.93
	12 storey	0.12	0.19	0.28	0.82	1.17	1.67
Reduced length BRB	3 storey	0.98	1.73	3.06	3.14	5.69	10.30
	6 storey	0.66	0.95	1.36	2.57	3.92	5.98
	9 storey	0.35	0.48	0.66	1.76	2.49	3.51
	12 storey	0.16	0.26	0.37	1.24	1.43	1.65

BRB: buckling-restrained brace.

Table 8. MAF of exceedance ($\times 10^{-4}$) for different limit states.

Limit state	3 storey		6 storey		9 storey		12 storey	
	IO	CP	IO	CP	IO	CP	IO	CP
Inverted-V – conventional BRB	1.516	2.152	1.560	2.822	0.118	0.140	0.077	0.102
Diagonal – conventional BRB	2.799	3.187	4.003	6.589	0.143	0.076	0.091	0.122
Inverted-V – reduced length BRB	0.900	1.742	1.409	2.053	0.042	0.146	0.211	0.214
diagonal-reduced length BRB	1.480	1.802	2.376	4.898	0.087	0.085	0.067	0.085

MAF: mean annual frequency; IO: immediate occupancy; CP: collapse prevention.

inverted-V BRBs. It means that at certain EDP levels, the MAF values are lower for reduced length BRB. However, MAF values are higher for reduced length BRB at higher EDP levels, especially in the vicinity of $\theta_{max} = 0.1$ (CP limit states). In other words, the return period (year) of a specific EDP is greater for diagonal and inverted-V (in about IO limit states) reduced length BRBFs. Consequently, their potential hazard probability values are lower than those of conventional ones. This is not so in the case of inverted-V BRBs in CP limit states. The return period (T_r) and probability of exceedance of 2% in 50 years were calculated for IO and CP limit states for all frames using Poisson distribution law (Faggella et al., 2013) and presented in Table 9 and Figure 15. It can clearly be seen in Figure 15(a) that the rates of occurrence in 50 years of IO limit states for the frames braced with reduced length BRBs are lower than those of conventional BRBs. It means that for this limit states, the

Figure 12. Simplified uniform hazard spectra of Tehran.

potential seismic hazard of the reduced length BRBFs is lower than that of conventional BRBFs. Based on Figure 15(b), the rates of occurrence in 50 years of CP limit states for diagonal-reduced length BRBFs are lower than those of conventional BRBFs (except 6-storey frame). However, these rates are higher in the

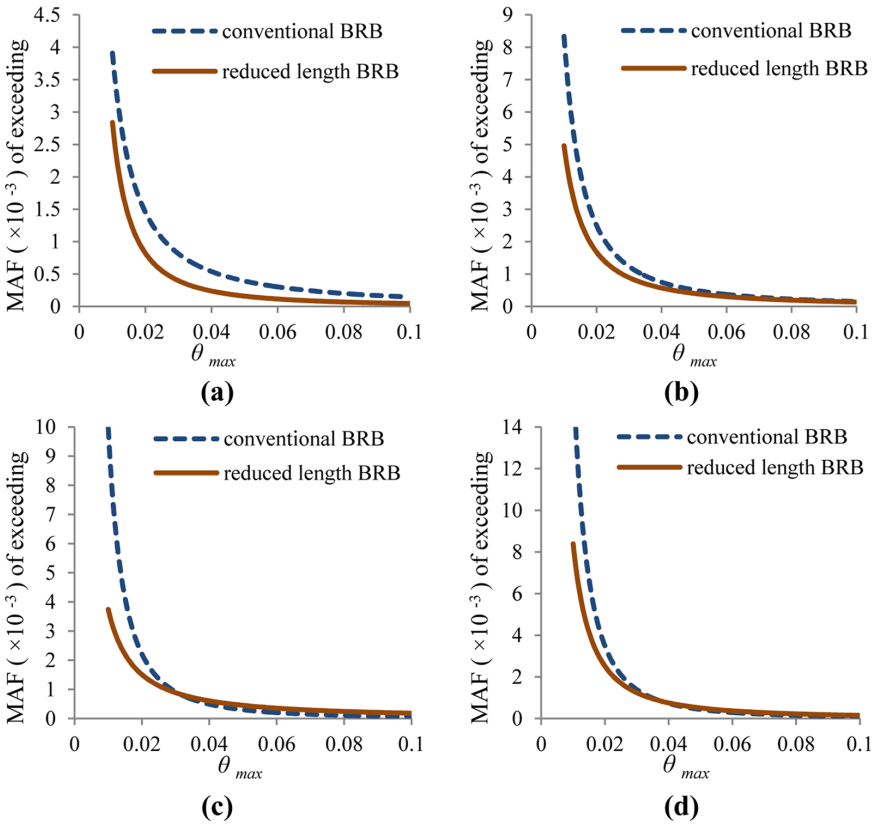

Figure 13. Seismic demand hazard curves of frames braced with inverted-V BRBs: (a) 3 storey, (b) 6 storey, (c) 9 storey and (d) 12 storey.

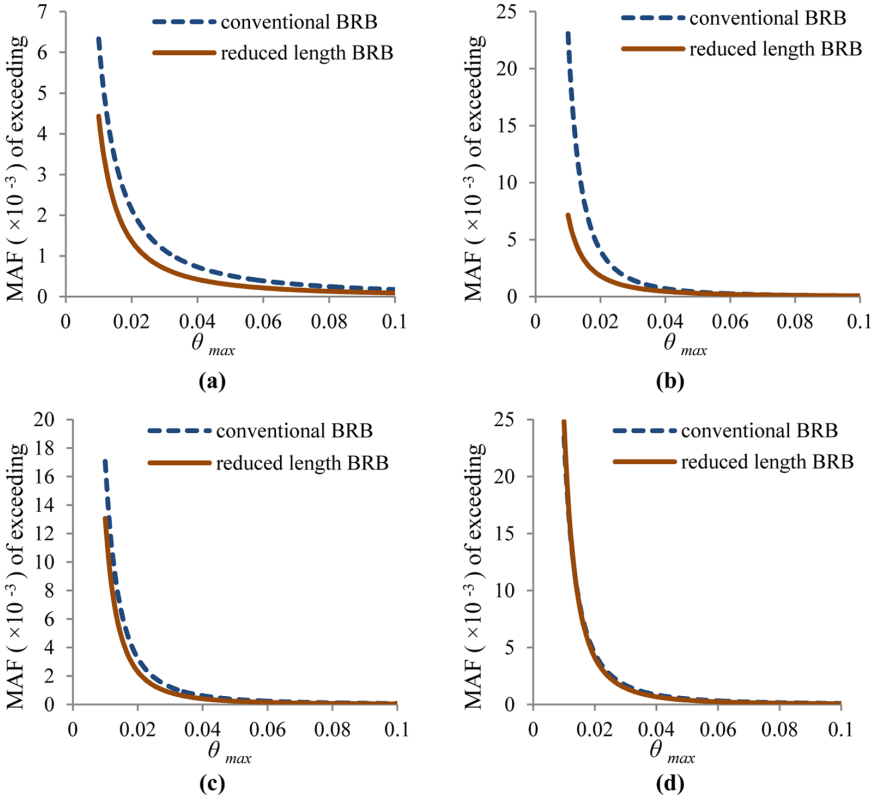

Figure 14. Seismic demand hazard curves of frames braced with diagonal BRBs: (a) 3 storey, (b) 6 storey, (c) 9 storey and (d) 12 storey.

Table 9. MAF, return period and probability of one time occurrence for 3-storey, 6-storey, 9-storey and 12-storey frames.

Bracing type	Conventional (inverted-V)		Reduced length (inverted-V)		Conventional (diagonal)		Reduced length (diagonal)	
Limit state	IO	CP	IO	CP	IO	CP	IO	CP
3-storey frames								
MAF	0.0015	0.0001	0.0009	0.0000	0.0028	0.0001	0.0015	0.0001
T_r (year)	659	8490	1112	23,886	357	6970	676	11,548
Probability of exceedance of 2% in 50 years (%)	**7.03**	**0.59**	**4.30**	**0.21**	**12.17**	**0.71**	**6.87**	**0.43**
6-storey frames								
MAF	0.0022	0.0001	0.0017	0.0001	0.0032	0.0001	0.0018	0.0001
T_r (year)	465	7159	574	6854	314	13,204	555	11,797
Probability of exceedance of 2% in 50 years (%)	**9.66**	**0.69**	**7.98**	**0.72**	**13.59**	**0.38**	**8.23**	**0.42**
9-storey frames								
MAF	0.0016	0.0001	0.0014	0.0002	0.0040	0.0001	0.0024	0.0001
T_r (year)	641	13,056	710	4745	250	11,038	421	14,988
Probability of exceedance of 2% in 50 years (%)	**7.22**	**0.38**	**6.56**	**1.04**	**16.38**	**0.45**	**10.55**	**0.33**
12-storey frames								
MAF	0.0028	0.0001	0.0021	0.0002	0.0066	0.0001	0.0049	0.0001
T_r (year)	354	9801	487	4682	152	8214	204	11,805
Probability of exceedance of 2% in 50 years (%)	**12.25**	**0.51**	**9.26**	**1.06**	**23.70**	**0.61**	**19.17**	**0.42**

MAF: mean annual frequency; IO: immediate occupancy; CP: collapse prevention.

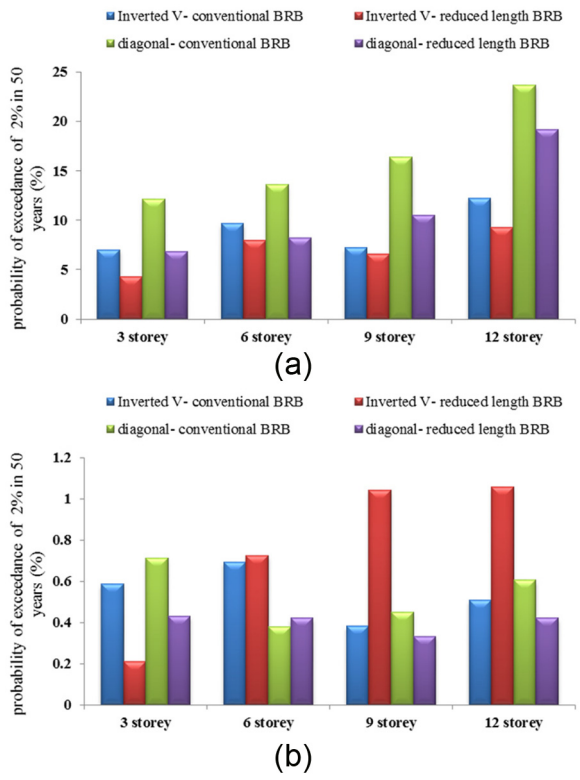

Figure 15. Probability of exceedance of 2% in 50 years for: (a) IO limit state and (b) CP limit state.

inverted-V – reduced length BRBF compared to those of conventional ones.

Conclusion

Since this study focuses on the probabilistic seismic performance of reduced yielding segment BRB with the details different from that of conventional BRB, the frames with 3, 6, 9 and 12 storeys were designed, modelled and analysed. They were braced with the two types of considered BRBs (reduced length and conventional) which have different configurations. The materials and geometry were assumed to be nonlinear. The frames were then subjected to a suite of 17 ground motion records for conducting IDA. The results of the analysis were used for estimating the performances of the frames in terms of *Sa* capacities for two limit statess: CP and IO. The *Sa* values corresponding to 16%, 50% and 84% failure probabilities were tabulated regarding different limit states of the frames with various heights. MAF of exceedance is derived for the two limit states through convolving fragility and seismic hazard curves. Additionally, the seismic demand hazard curves were plotted using PSDA approach. The values of MAF of exceedance were presented for different demand levels. These curves were generated considering the probabilistic content of seismic hazards. The remarks obtained by comparing the performances predicted by models with various heights are briefly summarized as follows:

- Regarding IDA curves, the reduced BRBFs have higher *Sa* capacities compared to conventional BRBFs;
- Comparing the fragilities obtained for the frames with various heights, the probability of failure is higher in taller buildings at a specific IM level;
- The probability of exceedance of IO limit states is lower in the reduced length BRBs compared to the conventional ones;
- The probability of exceedance of CP limit states is lower in diagonal-reduced length BRBs; however, this is not true for inverted-V BRBs;
- Further experimental studies are needed to demonstrate the advantages of reduced length BRB especially in CP limit states;
- The potential hazard probability of IO limit states for reduced length BRBFs is lower than that of conventional ones.

Declaration of Conflicting Interests

The author(s) declared no potential conflicts of interest with respect to the research, authorship and/or publication of this article.

Funding

The author(s) received no financial support for the research, authorship and/or publication of this article.

References

AISC 303-10 (2010) Code of standard practice for steel buildings and bridges.

American Institute of Steel Construction (AISC) (2005) *Seismic Provisions for Structural Steel Buildings*. Chicago, IL: AISC.

Ariyaratana C and Fahnestock LA (2011) Evaluation of buckling-restrained braced frame seismic performance considering reserve strength. *Engineering Structures* 33: 77–89.

Bai J and Ou J (2016) Earthquake-resistant design of buckling-restrained braced RC moment frames using performance-based plastic design method. *Engineering Structures* 107: 66–79.

BHRC Standard 2800 (2005) Iranian code of practice for seismic resistant design of buildings.

Choi KS, Park JY and Kim HJ (2017) Numerical investigation on design requirements for steel ordinary braced frames. *Engineering Structures* 137: 296–309.

Di Sarno L and Elnashai AS (2008) *Fundamentals of Earthquake Engineering*. Chichester: John Wiley & Sons.

Di Sarno L and Manfredi G (2010) Seismic retrofitting with buckling restrained braces: application to an existing non-ductile RC framed building. *Soil Dynamics and Earthquake Engineering* 33(11): 1279–1297.

Di Sarno L and Manfredi G (2012) Experimental tests on full-scale RC unretrofitted frame and retrofitted with buckling restrained braces. *Earthquake Engineering & Structural Dynamics* 41(2): 315–333.

Faggella M, Barbosa AR, Conte JP, et al. (2013) Probabilistic seismic response analysis of a 3-D reinforced concrete building. *Structural Safety* 44: 11–27.

Fanaie N and Afsar Dizaj E (2014) Response modification factor of the frames braced with reduced yielding segment BRB. *Structural Engineering and Mechanics: An International Journal* 50(1): 1–17.

Fanaie N and Ezzatshoar S (2014) Studying the seismic behavior of gate braced frames by incremental dynamic analysis (IDA). *Journal of Constructional Steel Research* 99: 111–120.

Jalali SA, Banazadeh M, Abolmaali A, et al. (2012) Probabilistic seismic demand assessment of steel moment frames with side-plate connections. *Scientia Iranica A* 19(1): 27–40.

Jalayer F and Cornell CA (2003) *A technical framework for probability-based demand and capacity factor design (DCFD) seismic formats*. PEER Report 2003/08. Berkeley, CA: Pacific Earthquake Engineering Research Center, University of California, Berkeley.

López WA and Sabelli R (2004) Seismic design of buckling-restrained braced frames. Steel tips, Structural Steel Educational Council, Moraga, CA, July.

Mahdavi Adeli M (2005) *Determination of uniform hazard spectrum and site specific design spectrum*. MSc Thesis, Amirkabir University of Technology, Tehran, Iran (in Persian).

Mahdavi Adeli M, Deylami A, Banazadeh M, et al. (2011) A Bayesian approach to construction of probabilistic seismic demand models for steel moment-resisting frames. *Scientia Iranica A* 18(4): 885–894.

Mahdavipour MA and Deylami A (2014) Probabilistic assessment of strain hardening ratio effect on residual deformation demands of Buckling-Restrained Braced Frames. *Engineering Structures* 81: 302–308.

Mazzolani F, Della Corte G and D'Aniello M (2009) Experimental analysis of steel dissipative bracing systems for seismic upgrading. *Journal of Civil Engineering and Management* 15: 7–19.

Mazzoni S, McKenna F, Scott, et al. (2007) *OpenSees Command Language Manual*. Berkeley, CA: Pacific Earthquake Engineering Research Center, University of California.

Menegotto M and Pinto PE (1973) *Method of analysis of cyclically loaded RC plane frames including changes in geometry and nonelastic behavior of elements under normal force and bending*. Preliminary report, IABSE, Zurich, vol. 13, pp. 15–22.

Miner MA (1945) Cumulative damage in fatigue. *Journal of Applied Mechanics* 12: 159–164.

Ministry of Housing and Urban Development (2008) *Iranian National Building Code, Part 10, Steel Structure Design*. Tehran, Iran: Ministry of Housing and Urban Development.

Mirghaderi R and Ahlehagh S (2008) Study of seismic behavior of SCBF with "balanced bracing". In: *Proceedings of the 14th world conference on earthquake engineering*, Bejing, China, 12–17 October 2008, Bejing, China: International Association for Earthquake Engineering.

Nakamura H, Maeda Y and Sasaki T (2000) *Fatigue Properties of Practical-Scale Unbonded Braces*. Tokyo, Japan: Architectural Institute of Japan.

Papailia A (2011) *Seismic fragility curves for reinforced concrete buildings*. MSc Thesis, University of Patras, Patras.

Razavi SA, Mirghaderi SR and Hosseini A (2014) Experimental and numerical developing of reduced length buckling-restrained braces. *Engineering Structures* 77: 143–160.

Razavi SA, Shemshadian ME, Mirghaderi SR, et al. (2011) Seismic design of buckling restrained braced frames with reduced core length. In: *Proceedings of the SEWC structural engineering world congress*, Como, 4–6 April.

Sehhati R (2008) *Probabilistic seismic demand analysis for the near-fault zone*. PhD Thesis, Department of Civil and Environmental Engineering, Washington State University, Pullman, WA.

Shemshadian ME, Razavi SA, Hosseini A, et al. (2011a) An analytical study of low cycle fatigue effects in buckling restrained braces. In: *Proceedings of the 3rd ECCOMAS thematic conference on computational methods in structural dynamics and earthquake engineering*, Corfu Greece, 25–28 May 2011.

Shemshadian ME, Razavi SA, Mirghaderi SR, et al. (2011b) The advantages of reducing the length of yielding segment in seismic performance of buckling restrained braced frames. In: *Proceedings of the sixth international conference of seismology and earthquake engineering*, Tehran, Iran, 16–18 May.

Shin DH and Kim HJ (2016) Influential properties of hysteretic energy dissipating devices on collapse capacities of frames. *Journal of Constructional Steel Research* 123: 93–105.

Tang Y and Zhang J (2011) Probabilistic seismic demand analysis of a slender RC shear wall considering soil–structure interaction effects. *Engineering Structures* 33(1): 218–229.

Titi A (2013) *Lifetime probabilistic seismic assessment of multistory precast buildings*. PhD Thesis, Doctoral School in Structural, Earthquake and Geotechnical Engineering, Department of Structural Engineering, Polytechnic University of Milan, Milan.

Tonekabonipour M (2013) *Probabilistic based seismic vulnerability assessment of RC frames*. PhD Thesis, Sharif University of Technology, Tehran, Iran (in Persian).

Tremblay R, Bolduc P, Neville R, et al. (2006) Seismic testing and performance of buckling restrained bracing system. *Canadian Journal of Civil Engineering* 33(2): 183–198.

Vamvatsikos D and Cornell CA (2002) Incremental dynamic analysis. *Earthquake Engineering & Structural Dynamics* 31(3): 491–514.

Watanabe A, Hitomi Y, Yaeki E, et al. (1988) Properties of brace encased in buckling-restraining concrete and steel tube. In: *Proceedings of the 9th world conference on earthquake engineering*, Tokyo-Kyoto, Japan, 2–9 August, vol. IV, pp. 719–724.